MODE II INTERLAMINAR FRACTURE OF GLASS/EPOXY MULTIDIRECTIONAL LAMINATES

A. B. Pereira[1], A. B. de Morais[1], A. T. Marques[2], P. T. de Castro[2]

[1]University of Aveiro, Department of Mechanical Engineering, Campus Santiago, 3810-193 Aveiro, Portugal.
[2]University of Porto, Faculty of Engineering, DEMEGI, Rua Dr. Roberto Frias, 4200-465 Porto, Portugal.

ABSTRACT

An experimental study was conducted on the mode II interlaminar fracture of woven fabric glass/epoxy multidirectional laminates. Selected specimen stacking sequences had starter delaminations in $\theta/-\theta$ and $0/\theta$ interfaces and their suitability for End-Notched Flexure (ENF) tests was first verified in Finite Element (FE) analyses. In contrast with previous studies on unidirectional laminates, G_{IIc} values measured from a mode II precrack were significantly higher than those from the film, thus revealing a pronounced *R*-curve effect. Initiation G_{IIc} values were found to increase slightly with the ply angle θ for both $\theta/-\theta$ and $0/\theta$ specimens. These results were interpreted in a subsequent FE analysis of interlaminar stresses ahead of the crack tip.

1. INTRODUCTION

Delamination is a particularly dangerous damage mode of high performance laminated composites. Therefore, considerable efforts have been devoted to the characterisation of delamination resistance, with a clear prevalence of Fracture Mechanics approaches [1,2]. The *Double Cantilever Beam* (DCB) test is nowadays standardised for the measurement of the mode I critical strain energy release rate, G_{Ic}, of unidirectional (UD) $[0^o]_n$ laminates [3-5]. On the other hand, various mode II specimens have been proposed but there is no consensus on which is the best one [6]. Nevertheless, owing to the simple set-up, the *End-Notched Flexure* (ENF, Fig. 1) test has been the most used [3,6].

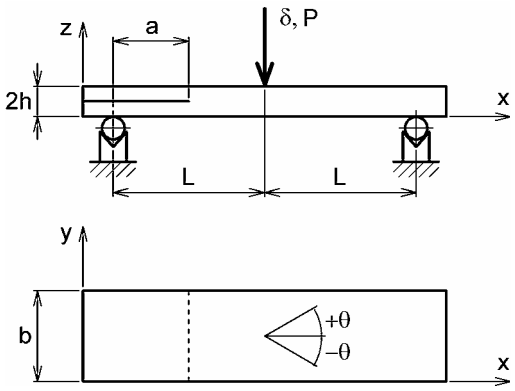

Fig. 1. The ENF specimen.

As in mode I, the ongoing pre-standardisation work has involved UD specimens, whose high stiffness and ability to sustain self-similar crack growth conditions are quite convenient for interlaminar fracture tests. However, most applications involve multidirectional (MD) laminates, and delaminations occur between plies of different orientations. Several studies were already performed on the mode II fracture of MD laminates [7-13]. The results are often contradictory e.g. G_{IIc} values reported for specimens with starter delaminations in $\theta/-\theta$ interfaces increased [7,8,10,11], decreased [13] or remained practically unaffected by the ply angle θ [9]. Actually, most of those results were affected by intraply damage and crack jumping to another interface. On the other hand, G_{IIc} values of $0/\theta$ specimens decreased with

θ [12,13], thus suggesting that UD specimens may not give the most conservative results. These unsolved questions motivated the study herein described.

2. SELECTION OF SPECIMEN STACKING SEQUENCES

When selecting stacking sequences for MD specimens, excessive elastic couplings that affect G_{IIc} measurements must be minimised. For example, bending-bending couplings may generate large anticlastic deformations and consequently highly curved delamination fronts and a considerable mode III component at the specimen edges [9,14,15]. In addition, bending-twisting and membrane-bending couplings are generally present in specimens having starter delaminations between differently oriented plies. Such couplings can induce unsymmetrical delamination fronts and significant effects of residual stresses on G_{IIc} measurements. On the other hand, MD laminates are not as stiff as UDs, and could be considerably tougher. Therefore, thick specimens should be used in order to avoid large displacements, plastic deformations and, if possible, intraply damage. These requirements lead to the choice of the following specimen stacking sequences [15,16]:

- $[(0_2/90)_6/0_2//(0_2/90)_6/0_2]$;
- $[(0_2/90)_6/0_2//\theta/(0_2/90)_6/0_2]$ with θ = 22.5 to 90 degrees;
- $[(0_2/90)_6/0_2/\theta//-\theta/(0_2/90)_6/0_2]$ with θ = 15 to 45 degrees;

where // denotes the position of the starter delamination. For convenience, the specimens are hereafter designated by the delaminating interface i.e. 0/0, 0/θ and $\theta/-\theta$. The incorporation of the thick symmetric $[(0_2/90)_6/0_2]$ block of 20 plies aimed at reducing the undesirable elastic couplings mentioned above.

The selected specimens were evaluated in a 3D FE analysis [15,16]. The specimen dimensions were (Fig. 1) width b = 20 mm, span $2L$ = 100 mm, crack length a = 25 mm [17] and total length 160 mm, while the thickness $2h$ varied from 6.0 to 6.3 mm as a result of the t = 0.15 mm ply thickness. The models were constructed with the commercial code ABAQUS® using 3D 8-node brick elements. Fig. 2 shows a typical FE mesh, which included the definition of contact surfaces to prevent interpenetration of the specimen arms. The models combined mesh refinement near the crack tip with the use of layered elements, in order to achieve accurate results without excessive computational cost.

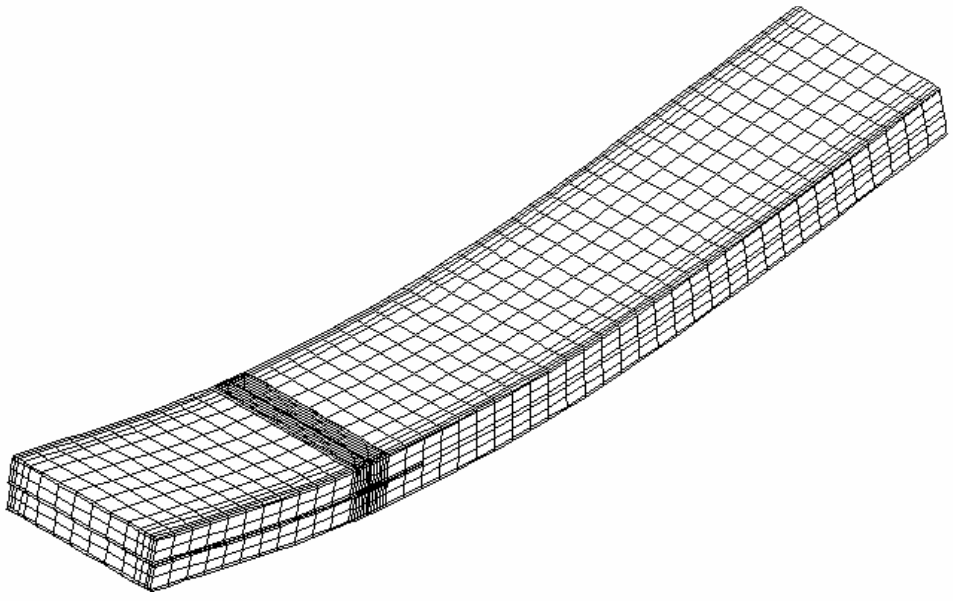

Fig. 2. Typical mesh of a FE model.

The Virtual Crack Closure Technique (VCCT) [18] was employed to compute the strain energy release rate components, G_{I}, G_{II} and G_{III}. It was shown that the stress field near delaminations between differently oriented plies is oscillatory, making mode partitioning somewhat dependent on the crack closure increment Δa [19,20]. This ambiguity can be avoided by considering Δa equal to a characteristic damage zone length of the order of the ply thickness t. Mode partitioning then becomes practically Δa-independent. The material used in this study was a crowsfoot satin woven fabric glass reinforced epoxy. The ply thermoelastic properties were $E_1 = 33$ GPa, $E_2 = 19$ GPa, $\nu_{12} = 0.17$, $G_{12} = 4.8$ GPa, $E_3 = 8$ GPa, $\nu_{13} = \nu_{23} = 0.33$, $G_{13} = G_{23} = 3$ GPa, $\alpha_1 = 8.0 \cdot 10^{-6}$ ºC^{-1}, $\alpha_2 = 20 \cdot 10^{-6}$ ºC^{-1} and $\alpha_3 = 24 \cdot 10^{-6}$ ºC^{-1}.

Fig. 3 shows the distributions of G_{II} along the width of 0/0, 0/45, 0/90 and 45/–45 specimens, which represent the limit cases of elastic couplings [14]. The distributions are quite uniform, apart from localised edge effects. Moreover, the mode-mixity results of Fig. 4 confirmed a high degree of mode II, the average mode II component being above 97 % of the total strain energy release rate $G = G_{\mathrm{I}} + G_{\mathrm{II}} + G_{\mathrm{III}}$.

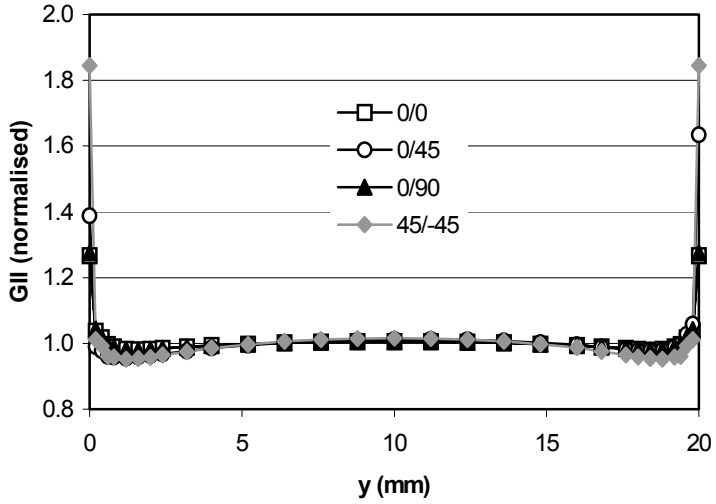

Fig. 3. Distributions of G_{II} along the width of ENF specimens. G_{II} values were normalised by the widthwise average.

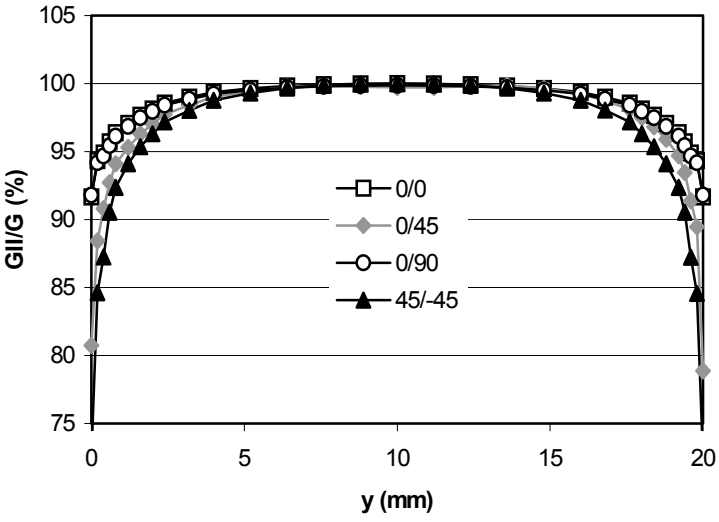

Fig. 4. Distributions of the mixed mode ratio G_{II}/G along the width of ENF specimens.

FE models were also used to assess the accuracy of the compliance calibration

$$C = C_0 + C_1 a + C_3 a^3 \tag{1}$$

leading to [21]

$$G_{II} = \frac{P^2}{2b}(C_1 + 3C_3 a^2) \tag{2}$$

where C_0, C_1 and C_3 are polynomial coefficients, P is the load, δ is the displacement and a = 15 to 35 mm. It was found that Eq. (1) fitted extremely well the original FE model compliance data (errors lower than 0.02 %), while the errors of Eq. (2) relative to VCCT were fairly small (table 1).

Table 1. Errors (%) of Eq. (2) relative to the original FE and VCCT results.

	a (mm)				
Specimen	15	20	25	30	35
0/0	1.09	0.59	0.80	1.17	1.55
0/45	1.90	1.41	1.66	2.06	2.48
0/90	1.40	0.78	0.98	1.33	1.74
45/-45	2.85	2.34	2.64	3.09	3.54

Finally, the influence of residual stresses on G_{II} was evaluated by performing a 100 ºC temperature decrease loading step. The results showed residual stresses played a minor role (table 2), even at the small width-wise average $G_{II} \approx 500$ J/m^2 assumed in this analysis. The effect of friction between the arms of the specimens was assessed by assuming a friction coefficient μ = 0.5. The differences relative to the non-friction case were lower than 0.6 % [16]. We could therefore conclude that the proposed specimens were adequate for ENF tests and that the above compliance calibration was a suitable data reduction scheme.

Table 2. Influence of residual stresses (RS) on the width-wise average G_{II}.

Specimen	G_{II} (normalised)		Error
	no RS	with RS	(%)
0/45	0.984	0.978	-0.56
0/90	0.990	1.000	1.01
45/-45	0.974	0.973	-0.18

3. EXPERIMENTAL

The laminated plates were prepared from a woven fabric glass/epoxy prepreg, reference EE190ET442, supplied by Texipreg. The fabric weave pattern was crowsfoot satin with 20 % fibres in the weft direction. A 15 μm thick PTFE film was used to generate the starter crack. The plates were manufactured by hot platen pressing according to the recommended processing conditions. Specimens were cut from the plates with the nominal dimensions of the FE models analysed. Tests were conducted at 1 mm/min crosshead speed on at least five specimens of each type. As in [12], 0/θ specimens were positioned on the ENF rig so that

compressive stresses acted on the θ-oriented plies, thus minimising the possibility of intraply cracking. Each specimen was subjected to preliminary flexural tests with a = 15, 20, 25, 30 and 35 mm in order to obtain compliance calibration data. A first ENF test enabled the measurement of G_{IIc} values from the insert and provided the precrack for the subsequent test. In all cases, no permanent deformations were visible after unloading. Owing to the difficulties in defining the exact instant of crack initiation, the non-linearity (NL) and the 5 % offset or maximum load criteria (5/M) [1,5,6,17] were used.

Figs. 5 and 6 present the average and scatter range of experimental G_{IIc} for both crack initiation criteria. Results are not given for 45/–45 specimens because the tensile loaded 45 degree plies failed prematurely, causing the delamination to jump to the neighbour 0/45 interface. It can be seen that G_{IIc} values from the film were significantly lower than those from the precrack, showing a pronounced R-curve effect. This contrasts with previous studies on unidirectional carbon-fibre and glass-fibre reinforced laminates [1,6,22]. Moreover, the difference between G_{IIc} values was higher when the NL criterion was employed. In fact, G_{IIc}(NL)/G_{IIc}(5/M) ratios were about 66 % from the film and 89 % from the precrack. It has been shown that the NL point may actually be associated with the onset of large displacements [1,22], but these were prevented by the high stiffness of the present specimens. Although visual observations are not considered reliable for defining initiation, they showed that crack initiation from the film was closer to the NL point, occurring under increasing loads. Therefore, the larger difference between G_{IIc}(NL) and G_{IIc}(5/M) from the film is due to the R-curve effect.

In spite of considerable scatter and of inevitable batch variations, G_{IIc} values tended to increase mildly with θ for both $\theta/-\theta$ and $0/\theta$ specimens (Figs. 5 and 6). Such interface dependence agrees with previous studies on $\theta/-\theta$ specimens in which intraply damage was absent [7,11]. However, an opposite trend was obtained in similar conditions by Tao and Sun [12] for carbon-epoxy $0/\theta$ specimens. Therefore, it was decided to perform an additional FE analysis concerning the interface effect on G_{IIc}.

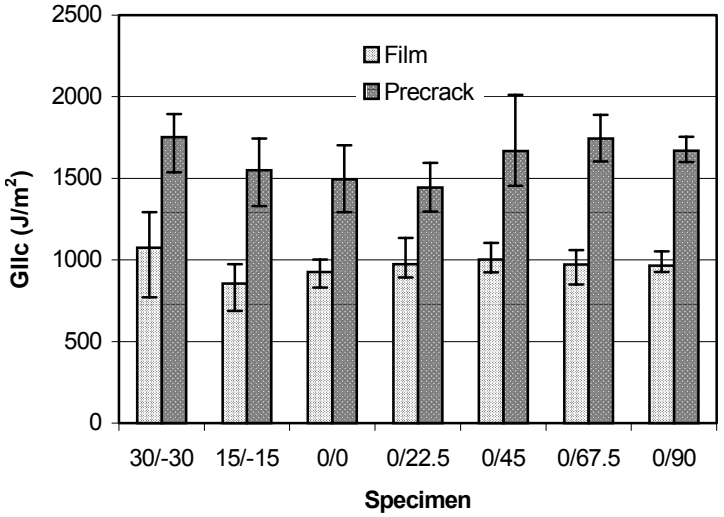

Fig. 5. Average G_{IIc} and scatter range obtained using the non-linearity (NL) criterion.

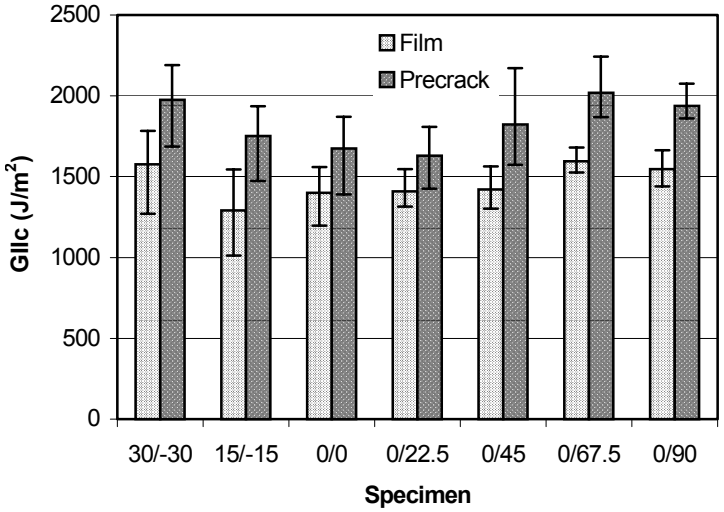

Fig. 6. Average G_{IIc} and scatter range obtained using the 5 % offset or maximum load (5/M) criterion.

4. INTERFACE EFFECT ON G_{IIc}

Fracture mechanics problems involving isotropic materials are commonly treated in terms of stress intensity factors K_j and fracture toughnesses K_{jc}, j being the loading mode. However, the delamination resistance of composites has been usually characterised by critical strain energy release rates, G_{jc}. One of the reasons is obviously the existence of fracture tests for the measurement of G_{jc} e.g. DCB, ENF and Mixed-Mode Bending (MMB). Another reason for preferring strain energy release rates is the greater difficulty in describing the stress field in the vicinity of the crack tip. The delamination between plies of different orientation is a particularly complex problem, in view of the oscillatory nature of the stress field [19,20]. As discussed above for strain energy release rates, mode partitioning usually requires "characteristic length stress intensity factors", which can only be evaluated by a complicated analytical treatment of numerical results [20]. Owing to the clear prevalence of mode II showed by the above FE analysis, it seemed appropriate to assume as good approximations the classical Fracture Mechanics relations [21]

$$\tau_{xz} \approx \frac{K_{II}(l_c)}{\sqrt{2\pi x}} \tag{3}$$

$$G_{II}(l_c) \approx \Psi K_{II}^2(l_c) \tag{4}$$

where τ_{xz} is the interlaminar shear stress, x is the horizontal distance measured from the crack tip and Ψ is a function of the specimen elastic constants. Obviously, the applicability of Eqs. (3) and (4) implies small oscillatory effects and thus mild l_c-dependence of K_{II} and G_{II}. Crack propagation can then be predicted when $G_{II}(l_c) = G_{IIc}$, or when $K_{II}(l_c) = K_{IIc}$. Eq. (4) allows us to express the ratio between G_{IIc} values of θ_1/θ_2 and 0/0 specimens by

$$\frac{G_{IIc}(\theta_1/\theta_2)}{G_{IIc}(0/0)} = \frac{\left[\frac{G_{II}}{K_{II}^2}\right](l_c,\theta_1/\theta_2)}{\left[\frac{G_{II}}{K_{II}^2}\right](l_c,0/0)} \frac{K_{IIc}^2(\theta_1/\theta_2)}{K_{IIc}^2(0/0)} \tag{5}$$

Furthermore, it can be easily deduced from Eq. (3) that

$$K_{\mathrm{II}} = \sqrt{\frac{\pi l_c}{2}}\,\bar{\tau}_{xz} \tag{6}$$

where $\bar{\tau}_{xz}$ is the l_c-averaged interlaminar shear stress, much easier to obtain from FE models than K_{II}. Therefore, Eq. (5) can be rewritten as

$$\frac{G_{\mathrm{IIc}}(\theta_1/\theta_2)}{G_{\mathrm{IIc}}(0/0)} = \lambda_{\mathrm{II}}\frac{K^2_{\mathrm{IIc}}(\theta_1/\theta_2)}{K^2_{\mathrm{IIc}}(0/0)} \tag{7}$$

where

$$\lambda_{\mathrm{II}} = \frac{\left[\dfrac{G_{\mathrm{II}}}{\bar{\tau}^2_{xz}}\right](l_c,\theta_1/\theta_2)}{\left[\dfrac{G_{\mathrm{II}}}{\bar{\tau}^2_{xz}}\right](l_c,0/0)} \tag{8}$$

In principle, λ_{II} should only depend on elastic constants i.e. $\lambda_{\mathrm{II}} = \psi(\theta_1/\theta_2)/\psi(0/0)$. At this stage, the difficulties in computing λ_{II} were the widthwise variations of G_{II} (Fig. 3) and $\bar{\tau}_{xz}$, and especially the computational cost inherent to 3D models. Actually, generalised plane strain (GPS) models were found to be good approximations to the average 3D results (table 3). This is partly due to the significant number of 90 degree plies of the specimen stacking sequences, which promoted low transverse membrane and anticlastic deformations.

Table 3. Differences (%) between generalised plane strain (GPS) and 3D FE models results for the compliance C and for G_{II}.

Specimen	a (mm)	C	G_{II}
0/0	15	-1.43	0.60
	25	-1.37	1.15
	35	-1.35	1.24
0/45	15	-1.46	1.74
	25	-1.50	1.86
	35	-1.57	1.94
0/90	15	-1.44	0.69
	25	-1.37	1.19
	35	-1.36	1.26
45/-45	15	-1.47	2.80
	25	-1.60	2.86
	35	-1.79	2.94

In order to obtain accurate λ_{II} ratios (8), very fine local meshing was employed i.e. the size of the elements near the crack tip was as small as $t/10$ in convergence studies. Fig. 7 shows that λ_{II} ratios (8) of $\theta/-\theta$ and $0/\theta$ specimens were not particularly sensitive to the exact l_c values of the order of the ply thickness, thus confirming the assumptions made in the above analytical developments.

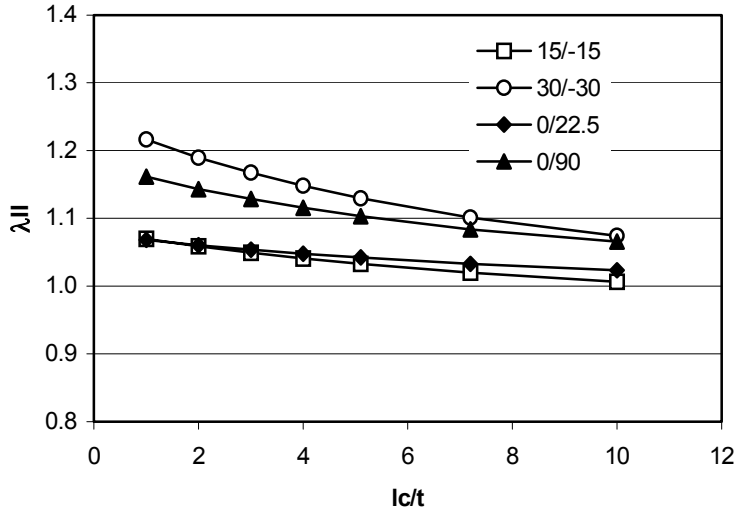

Fig. 7. Variation of λ_{II} ratios (8) with the characteristic length l_c.

Finally, using average experimental $G_{IIc}(0/0)$ and calculated λ_{II}, G_{IIc} values of other specimens were predicted. It can be seen in Figs. 8 and 9 that those predictions were in good agreement with the experimental results. Therefore, the interface dependency of G_{IIc} can be explained by the variation of the level of interlaminar shear stresses ahead of the crack tip, associated with the changes in specimen elastic properties. Accordingly, the present results suggest the existence of an interface independent fracture toughness K_{IIc}, probably resin controlled.

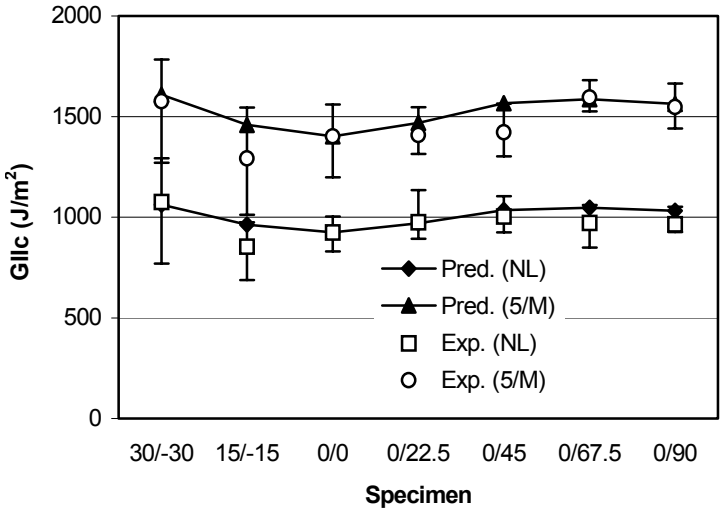

Fig. 8. Predictions of G_{IIc} based on calculated λ_{II} and on measured $G_{IIc}(0/0)$ from the film. ($l_c = 4t$ was used)

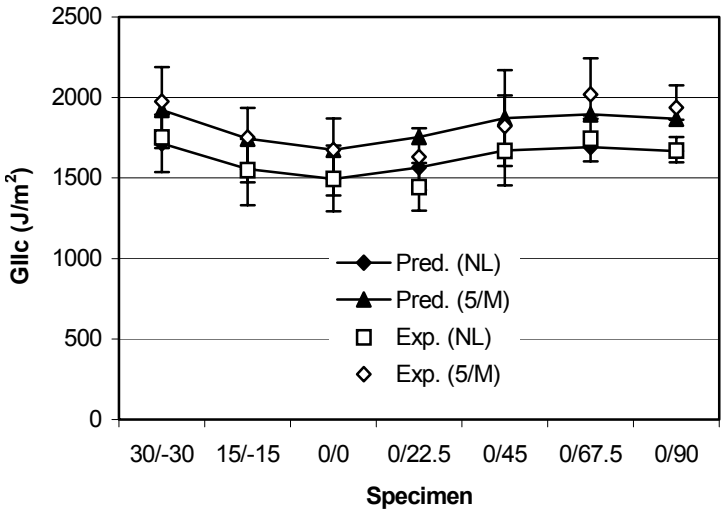

Fig. 9. Predictions of G_{IIc} based on calculated λ_{II} and on measured $G_{IIc}(0/0)$ from the precrack. ($l_c = 4t$ was used)

5. CONCLUSIONS

This paper described an experimental study on the mode II interlaminar fracture of woven fabric glass/epoxy multidirectional laminates. Specimen stacking sequences with starter delaminations in $\theta/-\theta$ and $0/\theta$ interfaces were chosen in order to avoid elastic couplings associated problems. Finite Element (FE) analyses were performed to evaluate the suitability of the selected specimens for End-Notched Flexure (ENF) tests and to validate a calibration data reduction scheme.

In order to avoid intraply damage, $0/\theta$ specimens were positioned on the testing rig so that the interfacial θ-oriented ply would be under compression. As to $\theta/-\theta$ specimens, premature intraply damage was absent for $\theta \leq 30$ degrees. Experimental G_{IIc} values increased slightly with θ for both $\theta/-\theta$ and $0/\theta$ specimens. In all cases, G_{IIc} values from the precrack were significantly higher than those from the film, revealing a pronounced *R*-curve effect.

An additional FE analysis was performed to interpret the interface effect on G_{IIc}. It was found that the interface dependency of G_{IIc} could be explained by the variation of the level of interlaminar shear stresses ahead of the crack tip, inherent to changes in specimen elastic properties. Therefore, the results suggest the existence of an interface independent fracture toughness K_{IIc}, probably resin controlled.

ACKNOWLEDGEMENTS

The authors thank the support of the Portuguese Foundation for Science and Technology (FCT, research project POCTI/EME/38731/2001, FEDER European Union fund).

References

1. **Davies, P., Blackman, B.R.K.** and **Brunner, A.J.**, "Standard test methods for delamination resistance of composite materials: current status", *Appl. Compos. Mater.*, **5** (1998), 345-364.
2. **Tay, T.E.**, "Characterization and analysis of delamination fracture in composites: an overview of developments from 1990 to 2001", *Appl. Mech. Rev.*, **56** (2003), 1-31.
3. JIS K 7086:1993, "Testing methods for interlaminar fracture toughness of carbon fibre reinforced plastics".

4. ASTM D 5528-94a, "Standard test method for mode I interlaminar fracture toughness of unidirectional fiber-reinforced polymer matrix composites", *Annual Book of ASTM Standards*, Vol. 15.03, American Society for Testing Materials, 2000.
5. ISO 15024:2001, "Fibre-reinforced plastic composites - Determination of mode I interlaminar fracture toughness, G_{Ic}, for unidirectionally reinforced materials".
6. **Davies, P., Sims, G.D., Blackman, B.R.K., Brunner, A.J., Kageyama, K., Hojo, M., Tanaka, K., Murri, G., Rousseau, C., Gieseke, B.** and **Martin, R.H.**, "Comparison of test configurations for determination of mode II interlaminar fracture toughness: results from international collaborative test programme", *Plastics, Rubber and Composites*, **28** (1999), 432-437.
7. **Chai, H.**, "Interlaminar shear fracture of laminated composites", *Int. J. Fract.*, **43** (1990), 117-131.
8. **Chou, I., Kimpara, I., Kageyama, K.** and **Ohsawa, I.**, "Mode I and mode II fracture toughness measured between differently oriented plies in graphite/epoxy composites", *Composite Materials: Fatigue and Fracture* - 5th Volume, ASTM STP 1230, 132-151, Philadelphia, 1995.
9. **Polaha, J.J., Davidson, B.D., Hudson, R.C.** and **Pieracci, A.**, "Effects of mode ratio, ply orientation and precracking on the delamination toughness of a laminated composite", *J. Reinf. Plast. Compos.*, **15** (1996), 141-173.
10. **Choi, N.S., Kinloch, A.J.** and **Williams, J.G.**, "Delamination fracture of multidirectional carbon-fiber/epoxy composites under mode I, mode II and mixed-mode I/II loading", *J. Compos. Mater.*, **33** (1999), 73-100.
11. **Ozdil, F., Carlsson, L.A.** and **Davies, P.**, "Beam analysis of angle-ply laminate end-notched flexure specimens", *Compos. Sci. Technol.*, **58** (1998), 1929-1938.
12. **Tao, J.X.** and **Sun, C.T**., "Influence of ply orientation on delamination in composite laminates", *J. Compos. Mater.*, **32** (1998), 1933-1947.
13. **Hwang, J.H., Kwon, O., Lee, C.S.** and **Hwang, W.**, "Interlaminar fracture and low velocity impact of carbon/epoxy composite materials", *Mech. Compos. Mater.*, **36** (2000), 195-214.
14. **Davidson, B.D., Krüger, R.** and **König, M.**, "Three dimensional analysis and resulting design recommendations for unidirectional and multidirectional end-notched flexure tests", *J. Compos. Mater.*, **29** (1995), 2108-2133.
15. **de Morais, A.B.**, "Analysis of mode II interlaminar fracture of multidirectional laminates", *Composites Part A*, **35** (2004), 51-57.
16. **Pereira, A.B.** and de **Morais, A.B.**, "Mode II interlaminar fracture of glass/epoxy multidirectional laminates", *Composites Part A*, **35** (2004), 265-272.
17. ESIS - Polymers & Composites Task group. Protocols for interlaminar fracture testing of composites. Edited by P. Davies, 1993.
18. **Shivakumar, K.N., Tan, P.W.** and **Newman, J.C.**, "A virtual crack-closure technique for calculating stress intensity factors for cracked three-dimensional bodies", *Int. J. Fract.*, **36** (1988), R43-R50.
19. **Raju, I.S., Crews, J.H.** and **Aminpour, M.A.**, "Convergence of strain energy release rate components for edge-delaminated composite laminates", *Engng. Fract. Mech.*, **30** (1988), 383-396.
20. **Chow, W.T.** and **Atluri, S.N.**, "Stress intensity factors as the fracture parameters for delamination crack growth in composite laminates", *Composites* **28B** (1997), 375-384.
21. **Kaninnen, M.F.** and **Popelar C.H.**, "Advanced Fracture Mechanics", Oxford University Press, New York, 1985.
22. **Davies, P., Ducept, F., Brunner, A.J., Blackman, B.** and **Morais, A.B.**, "Development of a standard mode II shear fracture test procedure", Proceedings of the 7th European Conference on Composite Materials (ECCM-7), Vol. 2, 9-18, London, May 1996.